Biochimica et Biophysica Acta 1798 (2010) 52–58

Contents lists available at ScienceDirect

Biochimica et Biophysica Acta

journal homepage: www.elsevier.com/locate/bbamem

A peptide based on the pore-forming domain of pro-apoptotic poliovirus 2B viroporin targets mitochondria

Vanesa Madan [a], Silvia Sánchez-Martínez [b,1], Luis Carrasco [a], José L. Nieva [b,*]

[a] Centro de Biología Molecular (CSIC-UAM), Universidad Autónoma de Madrid, Canto Blanco, 28049 Madrid, Spain
[b] Unidad de Biofísica (CSIC-UPV/EHU), Universidad del País Vasco, Aptdo. 644, 48080 Bilbao, Spain

ARTICLE INFO

Article history:
Received 14 September 2009
Received in revised form 14 October 2009
Accepted 21 October 2009
Available online 29 October 2009

Keywords:
Enterovirus 2B
Viroporin
Protein–lipid interaction
Pore-forming peptide
Viral protein-induced apoptosis

ABSTRACT

Non-structural poliovirus 2B protein induces plasma membrane permeabilization and has been recently implicated in triggering apoptosis via the mitochondrial pathway. Here we describe that the pore-forming P3 peptide, based on the 2B amphipathic domain, translocates through the plasma membrane of culture cells and targets mitochondria. Cell permeabilization by P3 versions of different lengths, together with peptide uptake analyses supported an internalization mechanism dependent on P3 capacity to interact physically with lipid bilayers and establish permeating pores therein. Internalized P3 was found associated with mitochondria, but contrary to the parental 2B protein, the short peptide did not affect the morphology or cell distribution of these organelles, nor induced apoptosis. We conclude that P3 constitutes a mitochondriotropic sequence, which is however devoid of 2B pro-apoptotic activity.

1. Introduction

The viroporin family includes viral proteins with potential membrane permeabilizing activity [1–4]. The poliovirus (PV) 2B product has been described as a prototypical member of this family [3,5]. PV 2B shares several structural characteristics with other viroporin members including its small size (less than 100 aa), the absence of glycosilation and a high degree of hydrophobicity [3]. This latter property enables 2B insertion into membranes as an integral product [5,6]. Upon membrane insertion, PV 2B tends to oligomerize assembling hydrophilic pores [7]. Recent functional analyses have revealed that viroporins could be further involved in the induction of an apoptotic response in mammalian cells during virus infection [8]. PV 2B expression from a Sindbis virus (SV) replicon induces degradation of internucleosomal DNA and generation of apoptotic bodies [8]. The expressed 2B product was partially associated with mitochondria and found to alter the normal morphology of these organelles. In addition, cytochrome c release and caspase-3 activation were evidenced upon 2B expression. It was therefore concluded that 2B triggers programmed cell death through the mitochondrial pathway.

In a more general sense, these observations imply that viroporins may represent a subset of the viral proapoptotic proteins that translocate into mitochondrial membranes and induce their permeabilization [9,10]. It has been pointed out that these proteins invariably contain amphipathic α-helices required for their activity and seem to have pore-forming properties [10]. According with this idea, the 2B sequence bears a Lys-based amphipathic domain (Fig. 1A), which is conserved among the members of the *Picornaviridae* family [5,6,11] and required for its interaction with cell and model membranes [2,5–7,11–13]. A peptide representing this sequence, designated as P3, was shown to effectively permeabilize the plasma membrane to small solutes when externally added to cultured cells, an activity that correlated with its capacity for establishing permeating pores in lipid vesicles [14]. Furthermore, conductance measurements of cells recorded in whole-cell configuration confirmed the assembly of ion-conducting P3 channels [14]. In view of the experimental evidence, it was concluded that this short peptide could mimic the pore-forming activity of 2B viroporin.

Currently proposed molecular mechanisms establish a link between pore-formation and peptide translocation across membranes, at least in some instances (see for reviews [15–19] and for extensive discussions [20,21]). In line with this postulate, we report here that the pore-forming P3 peptide efficiently translocates through the plasma membrane of culture cells. However, in contrast to the general trend followed by non-permeabilizing cell-penetrating peptides [18,22], or pore-forming mammalian antimicrobial peptides that translocate into cultured cells [23–26], the 2B-derived peptide displayed strong mitochondrial localization. This observation prompted us to assess further its capacity to mimic pro-apoptotic 2B activity. The confocal microscopy data indicated that P3 did not affect the mitochondrial morphology or cell distribution. Furthermore, this sequence was

* Corresponding author. Unidad de Biofísica (CSIC-UPV/EHU) and Departamento de Bioquímica y Biología Molecular, Universidad del País Vasco, Aptdo. 644, 48080 Bilbao, Spain. Tel.: +34 94 6013353; fax: +34 94 6013360.
E-mail address: gbpniesj@lg.ehu.es (J.L. Nieva).
[1] Present address: HIV Drug Resistance Program, National Cancer Institute, Frederick, MD 21702-1201, USA.

0005-2736/$ – see front matter © 2009 Elsevier B.V. All rights reserved.
doi:10.1016/j.bbamem.2009.10.013

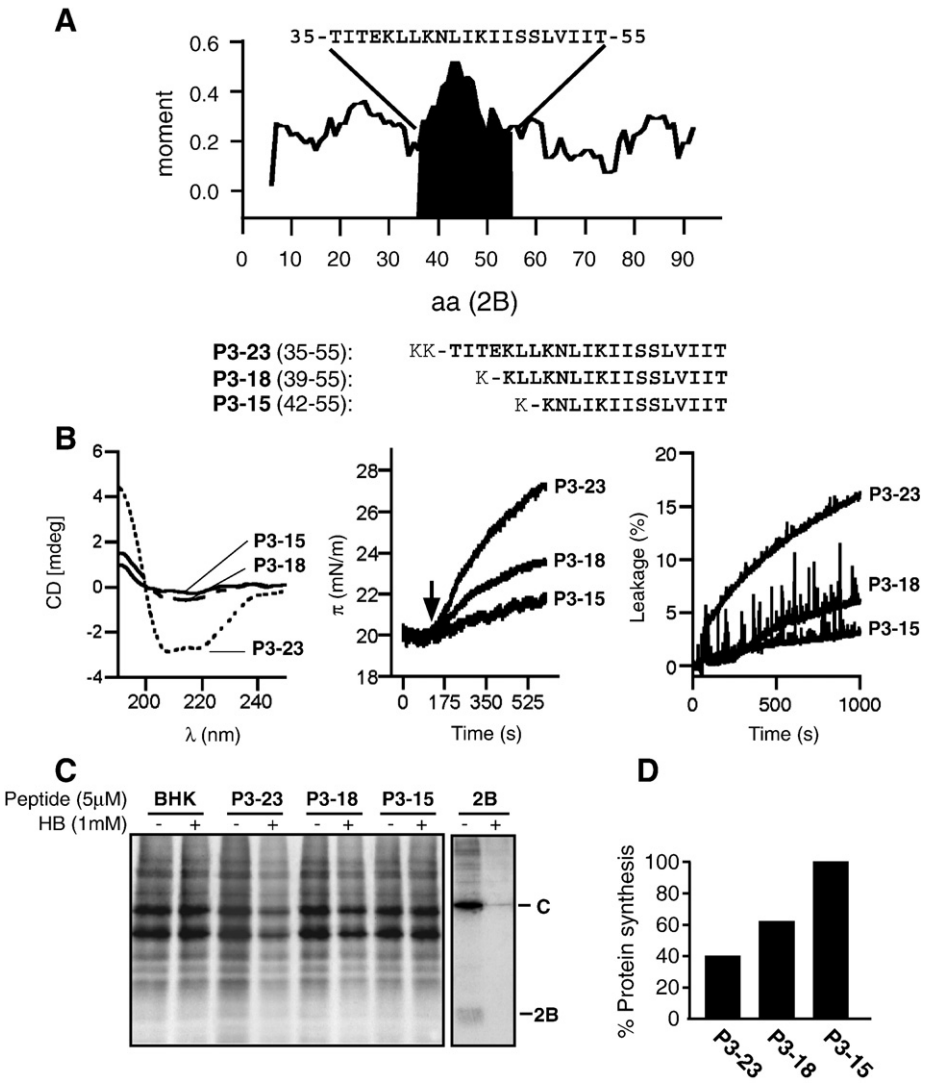

Fig. 1. Implication of the amphipathic sequence on membrane interactions and cell-permeabilizing capacities of P3. (A) PV 2B sequence hydrophobic moment in the α-helical conformation, calculated with a sliding window of 11 amino acids and Kyte–Doolitle hydrophobicity scale. The amphipathic domain (sequence above) spans the peak region colored in black. The sequences and designations of derived peptides used to assess membrane interactions and cell-permeabilizing activity are shown below. (B) Left: CD spectra of P3–23, P3–18 and P3–15 peptides in buffer containing 50 mM SDS. Center: increase of lateral surface pressure induced by peptide insertion into a phosphatidylcholine (PC) monolayer initially compressed at 20 mN/m. Peptides (0.5 μM) were injected into the subphase at the time indicated by the arrow. Right: kinetics of aqueous contents release from large unilamellar vesicles. Peptides (4 μM) were injected into a stirring solution of PC vesicles (100 μM) at time = 50 s. (C) Membrane permeabilization to translation inhibitor hygromycin B (HB) estimated from the reduction in protein synthesis. Left panel: cells were incubated with P3-23, P3-18 or P3–15 for 1 h before HB addition and then with [^{35}S]Met/Cys for 40 min in the presence of the antibiotic. Right panel: control disclosing membrane permeabilization induced by the 2B protein expressed from "repC + 2B" Sindbis virus (SV) replicon as previously described [34]. Most cells were efficiently transfected and so only the expression of the SV capsid protein (C) and 2B is detected. C expression does not affect membrane permeability as described previously. (D) Levels of cell permeabilization to HB induced by the different peptides for 1 h at a concentration of 5 μM, presented as protein synthesis reduction in HB-treated cells compared with that of untreated cells. The percentages of protein synthesis represent the mean of two experiments.

devoid of the capacity of inducing cytochrome *c* release or caspase-3 activation exhibited by the parental protein. Thus, this short peptide was not sufficient to recapitulate the pro-apoptotic effects of the full-length 2B protein. We conclude that P3 mimics only partially the 2B viroporin activity measured in cells.

2. Materials and methods

The poliovirus 2B-derived P3-15, P3-18, P3-23 (Fig. 1A) and P3-25 (Fig. 2A) peptides were produced by solid-phase synthesis using Fmoc chemistry as C-terminal carboxamides and purified by HPLC at the Proteomics Section of the University Pompeu-Fabra (Barcelona, Spain). 1-palmitoyl-2-oleoylphosphatidylcholine (PC) was purchased from Avanti Polar Lipids (Birmingham, AL, USA). The 8-aminonaphtalene-1,3,6-trisulfonic acid sodium salt (ANTS), p-xylenebis(pyridinium) bromide (DPX), Mitotracker Red CMH2Ros, Alexa 488-conjugated goat anti-mouse IgG and Alexa 594-conjugated goat anti-rabbit IgG were obtained from Molecular Probes (Junction City, OR, USA). Fluorescein-conjugated streptavidin (Strep-FITC) was supplied by Sigma (St. Louis, MO, USA). All other reagents were of analytical grade.

Circular dichroism and lipid monolayer measurements have been described in detail elsewhere [14]. Vesicle permeabilization was assayed following the ANTS/DPX method [27] as previously described [7,14]. For the cell permeabilization assays baby hamster kidney (BHK-21) cells were grown at 37 °C in Dulbecco's modified Eagle medium (DMEM) supplemented with 5% fetal calf serum (FCS) and non-essential amino acids. Peptide-induced membrane permeabilization was achieved by incubating BHK-21 cells with the peptides in FCS-free DMEM. Cells were subsequently treated with 1 mM hygromycin B (HB) for 20 min at 37 °C. Proteins were then radiolabeled for 40 min with 10 μCi of [^{35}S]Met-Cys (Promix; Amersham Pharmacia) as previously described [28]. Protein synthesis was analyzed by SDS-

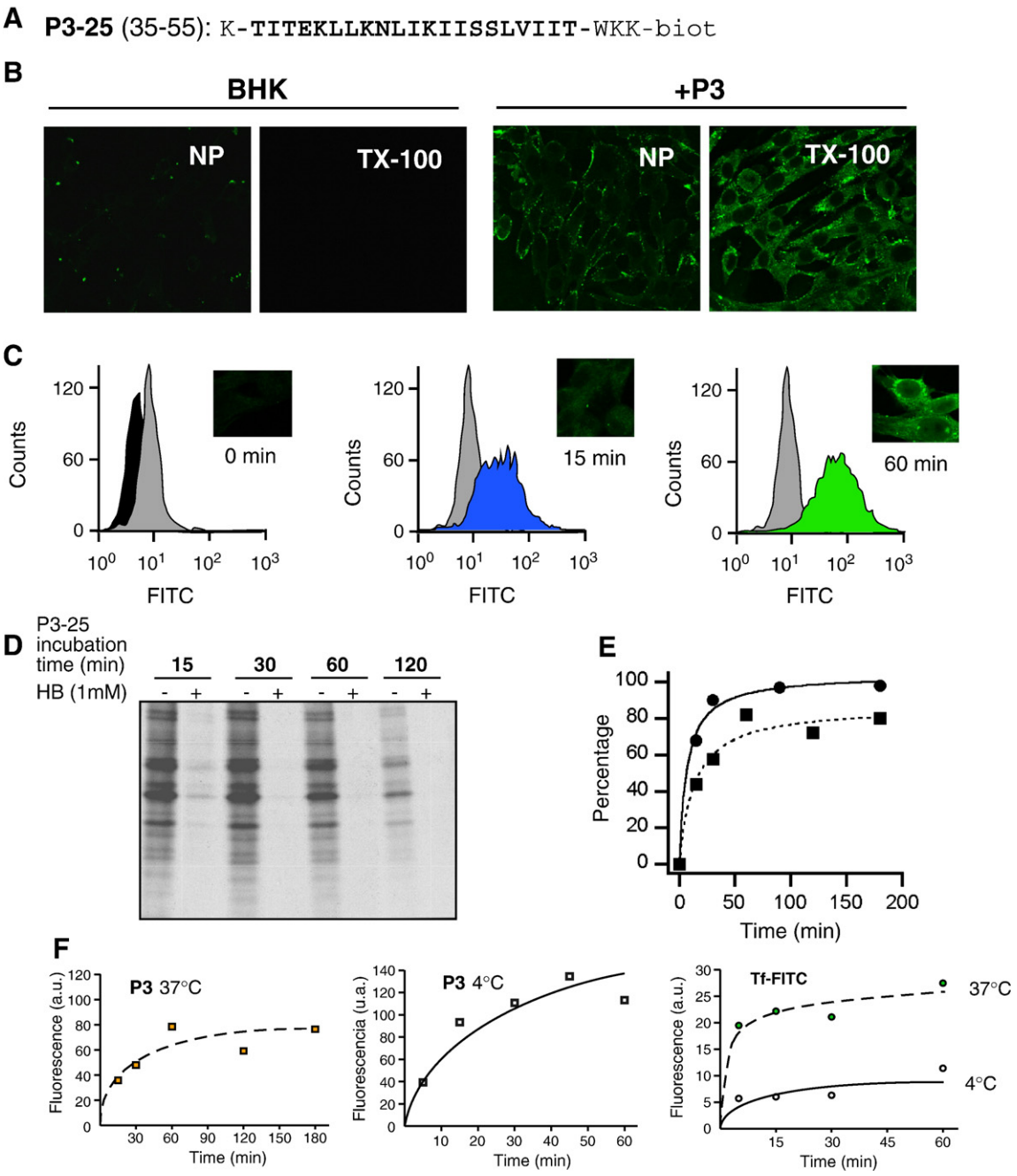

Fig. 2. Kinetics of P3-induced permeabilization and its internalization into BHK-21 cells. (A) Sequence of P3–25. (B) Binding to BHK-21 cell surface and internalization. Cells were treated with 1 μM P3–25 (+P3) for 1 h, or left untreated (BHK). After fixation, cells were labeled with Strep-FITC and analyzed in a confocal microscope (NP). Alternatively, the cells were permeabilized before Strep-FITC labeling (TX-100). (C) P3–25 internalization as a function of time. Histograms obtained by flow cytometry after incubating cells with 1 μM peptide are shown together with micrographs that illustrate the level of internal labeling at the different incubation times (insets). Black and gray controls correspond to untreated BHK cells and cells incubated with Strep-FITC alone, respectively. (D) Kinetics of cell membrane permeabilization to HB induced by 2.5 μM P3-25. (E) Levels of cell permeabilization (circles and solid line) and peptide internalization (squares and dotted line) as a function of time. The values represent, respectively, the percentage of HB-induced protein synthesis inhibition (panel D), and the percentage of cells emitting fluorescence above the background level (gray histogram in panel C). (F) P3-25 internalization at low temperature conditions. BHK cells were incubated in the presence of 1 μM P3–25 at 37 °C (left graph) or at 4 °C (middle graph) for the indicated periods of time. Transferrin-FITC (20 μg/ml) internalization by means of receptor-mediated endocytosis at 37 °C (green circles) or 4 °C (empty circles) served as a control for an energy-dependent entry mechanism (right graph). In both cases samples were treated with trypsin before FACS analysis.

PAGE and fluorography and quantified by densitometric scanning, using a GS-710 calibrated Imaging Densitometer (Bio-Rad).

For confocal microscopy, BHK-21 cells seeded on glass cover slips were incubated with biotinylated P3-25 peptide, extensively washed and fixed with 4% paraformaldehyde. Cells were subsequently washed twice in PBS, and then permeabilized for 10 min with 0.2% Triton X-100 in PBS. Incubations with Strep-FITC were carried out for 1 h in PBS containing 0.1% FCS and 0.1% TX-100. Specific rabbit policlonal antibodies against the PV 2B protein were diluted 1:300 and incubated for 1 h [29]. For mitochondria staining, cells were incubated with 2 μM Mitotracker Red for 45 min before fixation. For endosome co-localization experiments, a monoclonal antibody (MAb) against EEA1 (BD Transduction Laboratories) was diluted 1:200 and incubated for 1 h.

Flow cytometry samples consisted of P3-25-treated cells for different times at 37 °C or 4 °C that were washed and incubated with trypsin (0.05% in EDTA solution) for 5 min. FCS-containing PBS was added to the detached cells that were then centrifuged and washed twice in PBS-staining solution (1% bovine serum albumin, 1% FCS and 0.01% sodium azide in PBS). The cellular pellet was resuspended gently in 50 μl PBS-staining solution containing 0.3% saponin and 20 μg/ml Strep-FITC, and incubated at 4 °C for 20 min. Finally, cells were washed and resuspended in a PBS-staining solution containing 0.3 % saponin. Fluorescence analyses were performed with a BD FACScalibur Flow Cytometer (Becton Dickinson Immunocytometry Systems, Mountain View, CA). A minimum of 10,000 events per sample were included in the analyses.

In mitochondrial permeabilization assays, anti-cytochrome *c* MAb (BD Pharmingen; clone 6H2.B4) was diluted 1:100 and incubated for 2 h. Coverslips were washed three times with PBS between primary and secondary antibody incubations. Alexa 488- or Alexa 594-conjugated goat anti-mouse and anti-rabbit IgG were used as secondary antibodies. Coverslips were mounted in ProLong Gold antifade reagent (Invitrogen) and examined in a Radiance 2000 (Bio-Rad/Zeiss) confocal laser scanning microscope. Changes in nuclear morphology were assessed by DAPI (4′,6′-diamino-2-phenilindol) as described previously [8]. Images as those shown in Fig. 4C–F were acquired with a FRET microscope (Zeiss) using simultaneously fluorescence filters for Alexa 488, DAPI and phase contrast. The integrity of a caspase-3 substrate, eIF4GI (eukaryotic initiation factor 4GI), was analyzed by western blotting employing a rabbit anti-eIF4GI serum raised against peptides derived from the N- and C-terminal regions of human eIF4GI at a 1:1000 dilution. An anti-α-tubulin MAb (Sigma) was used at a 1:1000 dilution to evaluate protein loading.

3. Results and discussion

The PV 2B primary structure reveals the presence of 3 Lys residues dispersed with helical periodicity that is followed by a short stretch of hydrophobic amino acids (Fig. 1A, top) (see also references [6,11]). A previous screening of a complete 2B library identified a peptide based on this motif, designated as P3, which was capable of generating pore structures allowing passage of small solutes across the plasma membrane of cells growing in culture and boundary bilayers of lipid vesicles [14]. In order to get a deeper insight into the sequence requirements of this process, we first assessed the importance of the Lys-based amphipathic stretch for P3–membrane interactions and pore-forming activity. To that end we produced a series of peptides, P3–23, P3–18, and P3–15, which were truncated to different extents at the N-terminus of the P3 sequence (Fig. 1A, bottom).

The left panel of Fig. 1B displays the circular dichroism (CD) spectra of these peptides in the presence of SDS micelles. P3–23 adopted α-helical structure in solutions containing sodium dodecyl sulfate (SDS), consistent with its insertion into the membrane-mimicking detergent micelles. P3–18 exhibited a certain degree of structuring whereas P3–15 remained largely unstructured and/or aggregated. Lipid-monolayer and lipid vesicle experiments revealed that the former structuring behavior correlated with the capacity of these peptides for inserting into membranes and induce permeabilization (center and right panels, respectively). Thus, P3–23 increased lateral surface pressure of the lipid monolayer and induced release of the aqueous contents of lipid vesicles, but these effects were reduced for P3–18, and almost absent in the case of P3-15. Fig. 1C, D illustrate the abilities of these peptides to permeabilize cell monolayers. The fluorography analysis (panel C) shows as a control that single expression of 2B from a SV replicon induced protein synthesis inhibition in presence of the translation inhibitor hygromycin B (HB), a phenomenon reflecting the entry of this compound into permeabilized BHK-21 cells [8]. Addition of P3–23 to the culture medium also permeabilized cells to HB, thereby inducing 60% of protein synthesis inhibition (panel D). P3-18 inhibited protein synthesis to a lower extent (40%), whereas P3–15 had virtually no effect, as was the case for untreated controls.

Together, the results displayed in Fig. 1 reinforce the notion that P3 induces cell permeabilization by directly establishing pores in the plasma membrane, a process primarily mediated by the Lys-based amphipathic sequence. The presence of cationic residues is also a hallmark of many pore-forming peptides. According to the current view, pore-formation and peptide translocation across lipid bilayers might be coupled events in some instances [15,17–19]. The proposed models assume that peptides associated to the membrane external monolayer might assemble into peptide-rich domains, and cause a local imbalance across the bilayer in packing, surface tension and charge [20,21,30]. Translocation across the membrane would relieve such imbalance. This phenomenon is believed to occur through the formation of transient pores, which might vary in their lifetimes depending on the peptide species. Thus, within the framework of this theory, the permeating structures are considered as peptide-shuttling devices [17].

Therefore, we tested the possibility that P3 could translocate through the plasma membrane of cells and mark internal compartments (Fig. 2). For these experiments we used a P3 variant modified at the C-terminus, P3-25, which included an additional Trp residue, a 2 Lys-tag, and a biotin moiety (Fig. 2A). The inclusion of the fluorescent Trp residue allowed establishing in POPC vesicles a water–membrane partitioning constant, K_x, in the order of 10^6 (data not shown). This value lies in the range of that described for other natural pore-forming peptides such as melittin [31,32], and confirms that P3–25 is endowed with a comparable capacity for partitioning from water into lipid bilayers.

On the other hand, the biotin label allowed fluorescent detection of P3–25 by means of Strep-FITC binding. Confocal microscopy of samples treated with the peptide disclosed a fluorescent labeling at the periphery of the cells, consistent with peptides localized at the cell surface (NP in Fig. 2B, right). However, further cell permeabilization revealed an additional intracellular fluorescent labeling (TX-100 in Fig. 2B, right), which was absent from peptide-untreated control cells processed otherwise similarly (left panels). This internal labeling was observed within few minutes after peptide addition and reached its maximum after ca. 1 h. Similarly, most cells were by that time internally labeled according to flow cytometry determinations (Fig. 2C and E). Moreover, a strong signal of internalized peptide was already recovered after 15 min of incubation with peptide (Fig. 2C, insets). Results in Fig. 2D indicate that a great fraction of cells in culture were also permeable to HB under those conditions. Fig. 2E compares peptide-induced permeabilization to HB and internal labeling as a function of time. The data suggest that both processes followed parallel kinetics.

Flow cytometry assays were subsequently carried out to determine whether the peptide uptake process was dependent on active transport (Fig. 2F). P3-25 was observed to penetrate into BHK cells efficiently at 37 and 4 °C (left and center panels, respectively). In contrast, control experiments demonstrated that transferrin-FITC internalization via endocytosis was inhibited at 4 °C in the same system (right panel). Supporting an energy-independent translocation mechanism, P3-25 was also observed to localize intracellularly upon cell ATP depletion, while its internalization kinetics paralleled that measured in metabolically active cells (data not shown). Thus, collectively, the findings described in Fig. 2 provide evidence for the existence of a correlation between peptide internalization and pore-formation processes.

A closer inspection to the micrographs obtained by confocal fluorescence microscopy revealed Strep-FITC labeling of filiform structures (Fig. 3). This pattern suggested that internalized P3-25 might localize in mitochondria. Putative mitochondrial localization of P3–25 was therefore assessed by testing its colocalization with

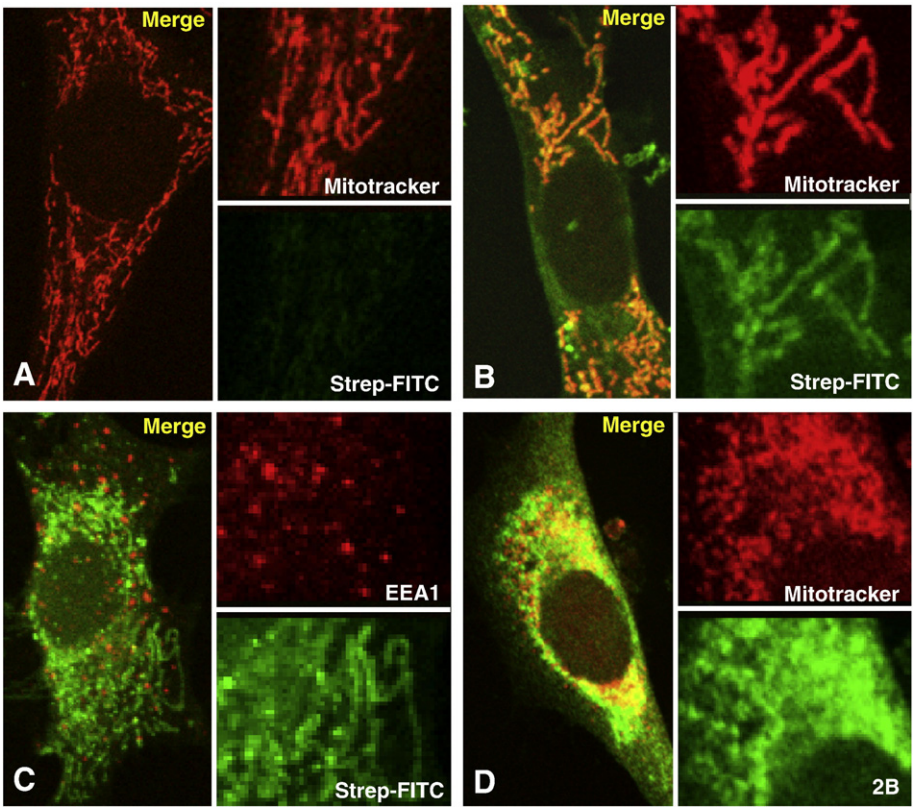

Fig. 3. Localization of internalized P3 peptide by confocal microscopy. (A) BHK cell staining with mitochondrial marker Mitotracker-Red and Strep-FITC in the absence of peptide. (B) Colocalization of P3-25 with Mitotracker-Red. Cells were treated with P3-25 (1 μM) for 3 h and incubated with Mitotracker-Red before fixation. Next, cells were permeabilized and stained with Strep-FITC. (C) Absence of colocalization of P3-25 with the endosomal marker anti-EEA1 (Early Endosome antigen 1) antibody. Conditions otherwise as in the previous panel. (D) Colocalization of PV 2B with Mitotracker-Red. Cells electroporated with a SV replicon construct coding for 2B protein [8] were incubated with the organelle marker. At 8 h after transfection, cells were permeabilized and stained with anti-2B antibody.

Mitotracker Red (Fig. 3A). Fig. 3B illustrates the fact that Mitotracker Red and Strep-FITC labeled similar elongated structures within P3-treated cells. Both markers colocalization in these samples was subsequently calculated with the Metamorph software [33]. This analysis rendered coefficients higher than 0.8 for the Mitotracker Red vs. Strep-FITC fluorescence intensity correlation (not shown). Fig. 3C displays a control experiment of colocalization of Strep-FITC with an endosomal marker (anti-EEA-1 antibody). Analysis of these samples rendered by comparison much lower correlation coefficients of ca. 0.1. The confocal microscopy experiments also revealed that the cell distribution and elongated morphology of mitochondria were similar in control cells without peptide and in peptide-treated cells (panels A and B, respectively). In sharp contrast, Mitotraker Red and the full-length 2B protein expressed from a SV-replicon appeared in micrographs obtained by confocal microscopy associated with punctate entities (Fig. 3D). The reorganization of the mitochondrial network induced by 2B expression was also evident in these micrographs. This phenomenon resulted in the accumulation of these organelles around the nucleus.

Overall, the experimental data displayed in Fig. 3 support a preferential P3–25 association with mitochondria. However, contrary to the parental 2B protein, the peptide did not induce the morphological changes that usually accompany mitochondrial membrane disruption. The results shown in Fig. 4 further confirmed that the P3–25 fraction associated to mitochondria was devoid of the pro-apoptotic activity exhibited by the parental 2B protein. The mitochondrial P3–25 did not increase external membrane permeability to cytochrome *c*, as judged from the absence of release of this apoptogenic compound into the cytoplasm of peptide-treated cells (Fig. 4A, top). This was again in contrast to the cytochrome *c* spilling observed in cells expressing the complete 2B protein (Fig. 4A, bottom). In line with an absence of apoptosis, cells treated with P3–25 did not exhibit eIF4GI cleavage (Fig. 4B), an evidence of caspase-3 activation that can be observed upon PV 2B expression [8].

As described earlier, the peptide internalization process leveled off within the first hour upon exposure (Fig. 2). After 4 h incubation, no apoptotic signals were evident in the peptide-treated cells. However, prolonged incubations with the peptide led to mitochondrial swelling (Fig. 4E, G). Yet, the cells displaying this abnormal mitochondrial morphology did not exhibit symptoms of cytochrome *c* release or nuclear fragmentation (compare with positive control STS-treated cells shown in Fig. 4C). Whether this effect was mediated by the mitochondria-associated peptide fraction, or else the consequence of the long-lasting plasma membrane permeabilization is difficult to ascertain. With even longer incubation periods the peptide toxicity was evidenced by the appearance of rounded cells mostly detached from the substrate (Fig. 4F). Nevertheless, no evidence of P3–25-induced apoptosis could be observed even under those conditions of long exposure to peptide.

3.1. Concluding remarks

Our previous characterization led us to propose P3 as a “one-helix” 2B version, which possessed the intrinsic capacity to permeabilize the cell plasma membrane [14]. Accordingly, we speculated that P3-induced cell permeabilization could be utilized in high-throughput screenings to identify viroporin inhibitors, which might in turn result useful leads for the development of new anti-viral compounds. The data reported here add to this notion that the P3 pore-forming activity: (i) requires the preservation of the Lys-based amphipathic domain (Fig. 1), and (ii) results in P3 internalization (Fig. 2).

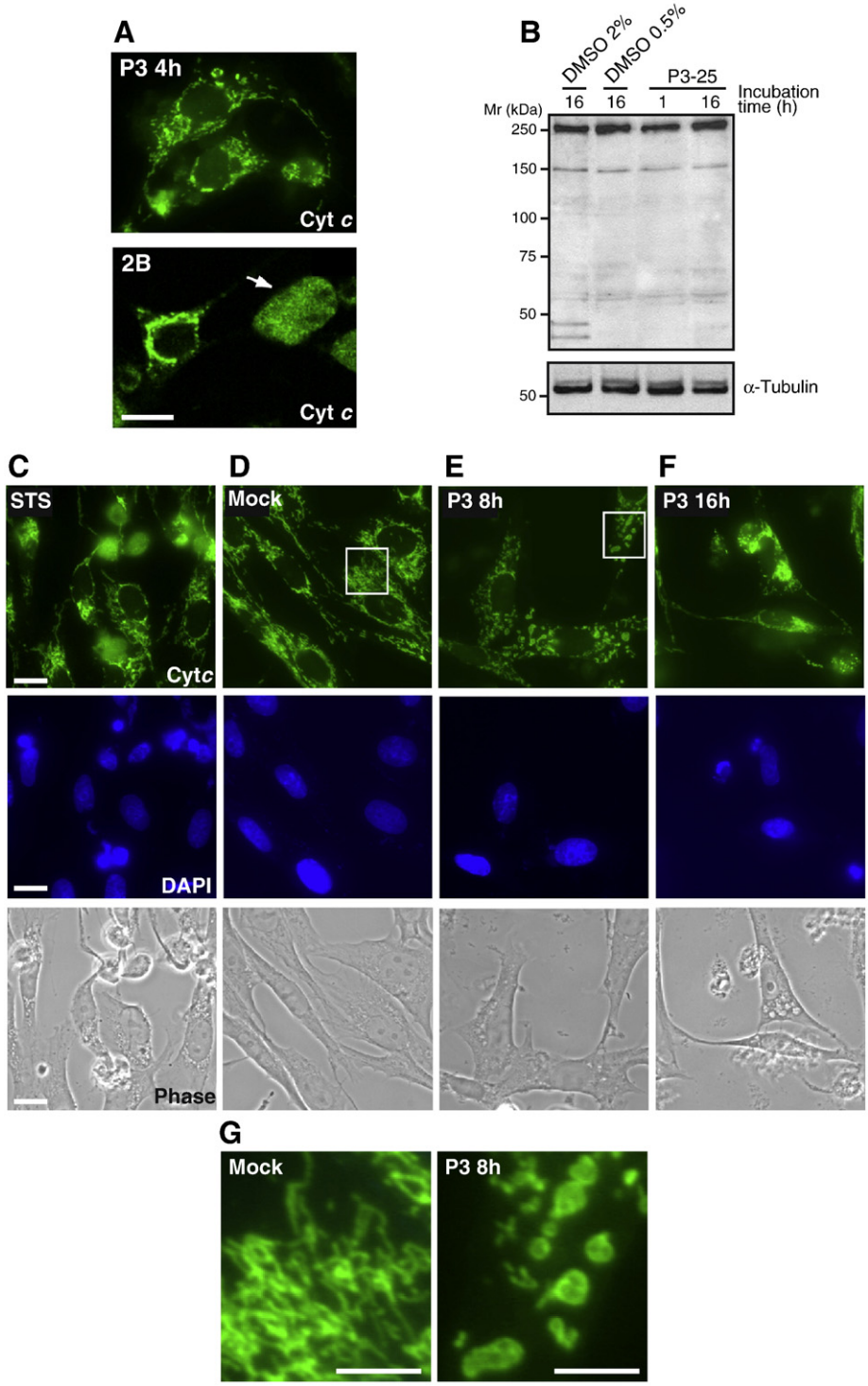

Fig. 4. Absence of P3 pro-apoptotic activity. (A) Cytochrome *c* release assay. Top: cells were fixed after incubation with peptide (1 μM) for 4 h, permeabilized and incubated with anti-cytochrome *c* antibody (cyt *c*). The micrographs display discrete labeling of mitochondria. Bottom: cells expressing PV 2B protein served as positive controls for cytochrome *c* efflux, which is detected as a fluorescent homogenous staining throughout the cytoplasm (arrow). (B) eIF4GI cleavage assay for caspase-3 activity. BHK cells were incubated with the peptide for 1 or 16 h, lysated and subjected to SDS-PAGE. A western blotting was performed using a polyclonal anti-eIF4GI antibody. Cells treated with 2 and 0.5% DMSO for 16 h served as positive and negative controls of apoptosis, respectively. Two typical eIF4GI cleavage products (below 50 kDa marker) by caspase-3 are detected only after incubation with 2% DMSO. A western blotting using monoclonal antibodies against α-tubulin was performed as a control of protein load. (C–F) Effect of P3-25 on nuclei and mitochondria integrity. Mitochondria morphology and cytochrome *c* release were assessed in mock cells (panel D) and cells treated with peptide for 8 and 16 h (panels E and F, respectively) using the anti-cytochrome *c* antibody (upper panels). Panel C displays a positive control for cytochrome *c* release that corresponds to cells incubated for 23 h with 1 μM staurosporine (STS). Nuclei were simultaneously stained with DAPI (middle panels) as described in Material and methods. Corresponding phase contrast images are shown in the lower panels. Bars, 10 μm. (G) Mitochondrial morphology in mock and P3- to 25-treated cells (right and left panels, respectively). Micrographs are amplified views of white boxes in panels D and E. Bars, 5 μm.

In addition to the plasma–membrane permeabilizing activity, the parental PV 2B protein has been recently described to induce apoptosis via the mitochondrial pathway [8]. This novel effect was proposed to represent an efficient mechanism to spread newly assembled virions, evading host immune inflammatory responses during the late phases of poliovirus infection. In spite of the encouraging finding that a major P3

fraction appeared associated with mitochondria (Fig. 3), the internalized peptide was unable to recapitulate the pro-apoptotic effects of 2B (Fig. 4). Taken together, the experimental evidence reported herein suggests that the short P3 peptide mimics only partially the activity displayed by 2B viroporin expressed in cells.

Acknowledgments

We acknowledge the financial support of DGICYT and MCINN Grants (BFU 2006-02182 and BIO 2008-00772). Further support to JLN was obtained from the Basque Government (AE2004-1-2) and the University of the Basque Country (GIU 06/42 and DIPE08/12). The Centro de Biología Molecular was awarded an institutional Grant by the Fundación Ramón Areces.

References

[1] L. Carrasco, L. Perez, A. Irurzun, F. Martinez-Abarca, P. Rodriguez, R. Guinea, J.L. Castrillo, M.A. Sanz, M.J. Ayala, in: L. Carrasco, N. Sonenberg, E. Wimmer (Eds.), Regulation of gene expression in animal viruses, Plenum Press, London, 1993, pp. 283–305.
[2] L. Carrasco, R. Guinea, A. Irurzun, A. Barco, in: B.L. Semler, E. Wimmer (Eds.), Molecular biology of picornavirus, ASM Press, Washington, 2002, pp. 337–354.
[3] M.E. Gonzalez, L. Carrasco, Viroporins, FEBS Lett. 552 (2003) 28–34.
[4] V. Madan, J. Garcia Mde, M.A. Sanz, L. Carrasco, Viroporin activity of murine hepatitis virus E protein, FEBS Lett. 579 (2005) 3607–3612.
[5] J.L. Nieva, A. Agirre, S. Nir, L. Carrasco, Mechanisms of membrane permeabilization by picornavirus 2B viroporin, FEBS Lett. 552 (2003) 68–73.
[6] F.J. van Kuppeveld, W.J. Melchers, K. Kirkegaard, J.R. Doedens, Structure–function analysis of coxsackie B3 virus protein 2B, Virology 227 (1997) 111–118.
[7] A. Agirre, A. Barco, L. Carrasco, J.L. Nieva, Viroporin-mediated membrane permeabilization. Pore formation by nonstructural poliovirus 2B protein, J. Biol. Chem. 277 (2002) 40434–40441.
[8] V. Madan, A. Castello, L. Carrasco, Viroporins from RNA viruses induce caspase-dependent apoptosis, Cell Microbiol. 10 (2008) 437–451.
[9] P. Boya, T. Roumier, K. Andreau, R.A. Gonzalez-Polo, N. Zamzami, M. Castedo, G. Kroemer, Mitochondrion-targeted apoptosis regulators of viral origin, Biochem. Biophys. Res. Commun. 304 (2003) 575–581.
[10] P. Boya, A.L. Pauleau, D. Poncet, R.A. Gonzalez-Polo, N. Zamzami, G. Kroemer, Viral proteins targeting mitochondria: controlling cell death, Biochim. Biophys. Acta 1659 (2004) 178–189.
[11] F.J. van Kuppeveld, J.M. Galama, J. Zoll, P.J. van den Hurk, W.J. Melchers, Coxsackie B3 virus protein 2B contains cationic amphipathic helix that is required for viral RNA replication, J. Virol. 70 (1996) 3876–3886.
[12] A.S. de Jong, W.J. Melchers, D.H. Glaudemans, P.H. Willems, F.J. van Kuppeveld, Mutational analysis of different regions in the coxsackievirus 2B protein: requirements for homo-multimerization, membrane permeabilization, subcellular localization, and virus replication, J. Biol. Chem. 279 (2004) 19924–19935.
[13] S. Sanchez-Martinez, N. Huarte, R. Maeso, V. Madan, L. Carrasco, J.L. Nieva, Functional and structural characterization of 2B viroporin membranolytic domains, Biochemistry 47 (2008) 10731–10739.
[14] V. Madan, S. Sanchez-Martinez, N. Vedovato, G. Rispoli, L. Carrasco, J.L. Nieva, Plasma membrane-porating domain in poliovirus 2B protein. A short peptide mimics viroporin activity, J. Mol. Biol. 374 (2007) 951–964.
[15] K. Matsuzaki, Why and how are peptide-lipid interactions utilized for self-defense? Magainins and tachyplesins as archetypes, Biochim. Biophys. Acta 1462 (1999) 1–10.
[16] Y. Shai, Mechanism of the binding, insertion and destabilization of phospholipid bilayer membranes by alpha-helical antimicrobial and cell non-selective membrane-lytic peptides, Biochim. Biophys. Acta 1462 (1999) 55–70.
[17] D.I. Chan, E.J. Prenner, H.J. Vogel, Tryptophan- and arginine-rich antimicrobial peptides: structures and mechanisms of action, Biochim. Biophys. Acta 1758 (2006) 1184–1202.
[18] S.T. Henriques, M.N. Melo, M.A. Castanho, Cell-penetrating peptides and antimicrobial peptides: how different are they, Biochem. J. 399 (2006) 1–7.
[19] H.W. Huang, Molecular mechanism of antimicrobial peptides: the origin of cooperativity, Biochim. Biophys. Acta 1758 (2006) 1292–1302.
[20] A. Pokorny, P.F. Almeida, Kinetics of dye efflux and lipid flip-flop induced by delta-lysin in phosphatidylcholine vesicles and the mechanism of graded release by amphipathic, alpha-helical peptides, Biochemistry 43 (2004) 8846–8857.
[21] J.M. Rausch, J.R. Marks, R. Rathinakumar, W.C. Wimley, Beta-sheet pore-forming peptides selected from a rational combinatorial library: mechanism of pore formation in lipid vesicles and activity in biological membranes, Biochemistry 46 (2007) 12124–12139.
[22] M.C. Morris, S. Deshayes, F. Heitz, G. Divita, Cell-penetrating peptides: from molecular mechanisms to therapeutics, Biol. Cell 100 (2008) 201–217.
[23] Y.R. Chan, R.L. Gallo, PR-39, a syndecan-inducing antimicrobial peptide, binds and affects p130(Cas), J. Biol. Chem. 273 (1998) 28978–28985.
[24] K. Takeshima, A. Chikushi, K.K. Lee, S. Yonehara, K. Matsuzaki, Translocation of analogues of the antimicrobial peptides magainin and buforin across human cell membranes, J. Biol. Chem. 278 (2003) 1310–1315.
[25] Y.E. Lau, A. Rozek, M.G. Scott, D.L. Goosney, D.J. Davidson, R.E. Hancock, Interaction and cellular localization of the human host defense peptide LL-37 with lung epithelial cells, Infect Immun. 73 (2005) 583–591.
[26] L. Tomasinsig, B. Skerlavaj, N. Papo, B. Giabbai, Y. Shai, M. Zanetti, Mechanistic and functional studies of the interaction of a proline-rich antimicrobial peptide with mammalian cells, J. Biol. Chem. 281 (2006) 383–391.
[27] H. Ellens, J. Bentz, F.C. Szoka, H+- and Ca2+-induced fusion and destabilization of liposomes, Biochemistry 24 (1985) 3099–3106.
[28] V. Madan, M.A. Sanz, L. Carrasco, Requirement of the vesicular system for membrane permeabilization by Sindbis virus, Virology 332 (2005) 307–315.
[29] A. Barco, L. Carrasco, A human virus protein, poliovirus protein 2BC, induces membrane proliferation and blocks the exocytic pathway in the yeast *Saccharomyces cerevisiae*, EMBO J. 14 (1995) 3349–3364.
[30] K. Matsuzaki, O. Murase, N. Fujii, K. Miyajima, Translocation of a channel-forming antimicrobial peptide, magainin 2, across lipid bilayers by forming a pore, Biochemistry 34 (1995) 6521–6526.
[31] M.J. Gomara, S. Nir, J.L. Nieva, Effects of sphingomyelin on melittin pore formation, Biochim. Biophys. Acta 1612 (2003) 83–89.
[32] D. Allende, S.A. Simon, T.J. McIntosh, Melittin-induced bilayer leakage depends on lipid material properties: evidence for toroidal pores, Biophys. J. 88 (2005) 1828–1837.
[33] J.W. Comeau, S. Costantino, P.W. Wiseman, A guide to accurate fluorescence microscopy colocalization measurements, Biophys. J. 91 (2006) 4611–4622.
[34] M.A. Sanz, V. Madan, L. Carrasco, J.L. Nieva, Interfacial domains in Sindbis virus 6K protein. Detection and functional characterization, J. Biol. Chem. 278 (2003) 2051–2057.